BEAM SHAPING AND PERMANENT MAGNET QUADRUPOLE FOCUSING WITH APPLICATIONS TO THE PLASMA WAKEFIELD ACCELERATOR*

R. J. ENGLAND, J. B. ROSENZWEIG, G. TRAVISH, A. DOYURAN, O. WILLIAMS, AND B. O'SHEA

University of California, Los Angeles
Department of Phyics and Astronomy
Los Angeles, CA 90095, USA

D. ALESINI

Laboratori Nazionali di Frascati
Rome, Italy

It has recently been proposed to use a dispersionless translating section (dogleg) with sextupole correction magnets as a bunch compressor to create longitudinally shaped (linearly ramped) electron bunches. We discuss the experiment soon to be underway at the UCLA Neptune Linear Accelerator Laboratory to test this technique with the 300 pC, 13 MeV electron bunches produced by the Neptune S-Band photoinjector. The experiment will utilize a dipole-mode deflecting cavity, as a temporal diagnostic, and a final focus system of permanent magnet quadrupoles with field gradients of 110 T/m. We also discuss the potential scaling of this technique to bunches of high (i.e.>1nC) charge for the purpose of creating a suitable drive beam for the plasma wakefield accelerator, operating in the blowout regime.

1. Introduction

The blowout regime of the plasma wakefield accelerator (PWFA)[1] has been the subject of various recent experimental and theoretical investigations.[2,3,4] In this regime, a relativistic beam (the drive bunch) produces large-amplitude wake-fields in a plasma of density n_0 much less than the drive beam density n_b. The high charge of the drive bunch causes plasma electrons in its wake to be expelled from the beam path, producing

*This work is supported by the Department of Energy under grant number DE-FG03-92ER40693.

a rarified ion column behind the bunch. The blowout regime is of considerable interest due to the fact that the induced wake-fields in the ion column exhibit linear focusing and accelerating forces, making it a well-behaved regime for the acceleration of either a low-charge witness bunch (injected in the wake of the drive beam) or the tail of the drive beam itself. Because plasmas can support very high electromagnetic fields, the accelerating gradients in this scheme can in principle be on the order of tens of GV/m, which is more than an order of magnitude improvement over traditional RF-based accelerating structures.

The current profile of the drive beam has been shown by analytical models [5,6] and by 2D simulations [7] to be optimized in this type of scenario when it has the shape of a triangular "ramp", with the beam current rising linearly from head to tail, followed by a sharp drop to zero at the tail. The transformer ratio (a figure of merit for the PWFA obtained by dividing the peak accelerating field behind the bunch by the deccelerating field within the bunch) for such a drive bunch in a plasma of density n_0 is given by $R = k_p L$, where $k_p = \sqrt{4\pi n_0 e^2/m_e c^2}$ is the plasma wavenumber, L is the length of the drive bunch 'ramp.' [5] Consequently, the value of the transformer ratio can in principle exceed the maximal value ($R = 2$) for a symmetric bunch profile, so long as the length of the ramp exceeds two plasma skin depths ($L > 2k_p^{-1}$).

A beam dynamics experiment designed to generate relativistic bunches whose current profile approximates the ideal 'ramped' bunches is presently underway at the UCLA Neptune linear accelerator laboratory.[8] The scheme proposed for this experiment takes advantage of the RF curvature superimposed upon the longitudinal phase space distribution of the bunch when it is injected into the accelerating section behind the crest of the accelerating field. A sextupole-corrected translating section (or dogleg) is used to partially compress the resulting bunch (which has a positive chirp in energy vs. longiudinal coordinate z), producing a final beam with a current distribution resembling a triangular ramp. Simulation results of the longitudinal phase space distribution and current profile for the Neptune experiment, using the particle tracking code PARMELA [9], are shown in Fig. 1. Part (a) shows the chirped beam generated by the photoinjector gun and linac. The final distribution, after passing through the dogleg, is shown in parts (b) and (c) with sextupole magnets off and on respectively. The use of sextupole correctors in part (c) to remove the nonlinear second-order correlation between energy and longitudinal position results in an almost purely linear compression of the initial chirped phase space distribution, producing

a beam with a current profile that rises gradually from head to tail, followed by a sharp drop. This bunch shape approximates the optimal triangular ramp, and has been shown in 2D particle-in-cell simulations to be capable of producing transformer ratios greater than 2 when properly matched into a plasma.[8]

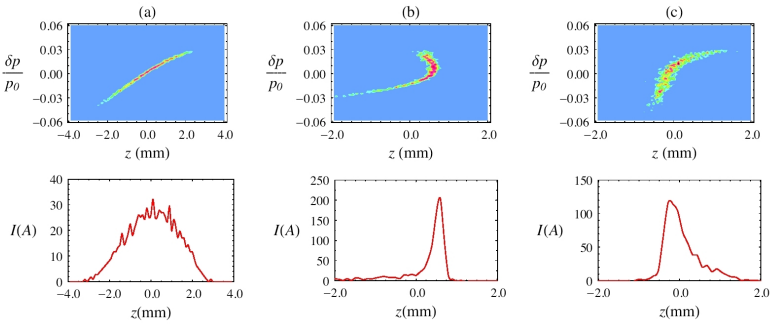

Figure 1. Simulated plots of longitudinal phase space and current profile for Neptune beam immediately after the accelerating section (a), and then after passing through the dogleg compressor with sextupoles turned off (b) and turned on (c).

To properly match such a beam into a plasma, we require that the betatron matching condition $\beta_r = \beta_{eq} = \sqrt{\gamma/(2\pi r_e n_0)}$ be satisfied, where γ is the normalized bunch energy, and r_e is the classical electron radius. From this requirement, combined with the previously mentioned condition on the bunch length L and the requirement for the blowout regime $n_b >> n_0$ (which we will interpret as $n_b > 4n_0$), we obtain a set of constraints on the plasma density, the drive beam RMS size σ_r, and the normalized emittance ϵ_N:

$$n_0 > n_{0,min} = \frac{mc^2}{\pi e^2 L}, \tag{1}$$

$$\sigma_r < \sigma_{max} = \sqrt{\frac{Q/e}{4\pi n_0 \sigma_z}}, \tag{2}$$

$$\epsilon_N < \epsilon_{N,max} = \gamma\beta\frac{\sigma_{max}^2}{\beta_{eq}}. \tag{3}$$

In these relations, we have approximated the beam density by $n_b = Q/(e\pi\sigma_r^2\sigma_z)$ and have used the definition of the normalized emittance

$\epsilon_N = \gamma\beta(\sigma_r^2/\beta_r)$, where β is the bunch velocity normalized by the speed of light, β_{eq} is the equilibrium beta function given above, σ_z is the RMS bunch length, and Q is the bunch charge. We can use these constraints to obtain the following expression for the minimum required beam brightness:

$$\mathcal{B} > \mathcal{B}_{min} = \frac{2cQ}{\epsilon_{N,max}^2 \sigma_z}. \quad (4)$$

Here we have used the definition for the transverse brightness $\mathcal{B} = 2I/\epsilon_N^2$, where $I = en_b\beta c\pi\sigma_r^2$ is the beam current. These relations provide us with an estimate of the required beam parameters for successfully applying the bunch shaping technique that is the subject of our experiment to create an adequate drive beam for a PWFA. In Section 2, we will compare these calculated threshold values with the simulated beam parameters for the Neptune experiment. In Section 3 we will consider possibilities for future experiments, including the creation of a witness bunch and scaling the Neptune experiment to high charge (4 nC).

2. UCLA Neptune Experiment

2.1. *Experimental Overview*

A cartoon of the experimental beamline is shown in Fig. 2. Electron bunches with an RMS bunch length of 2.5 ps are generated in the 1.6 cell S-Band photoinjector gun and are then accelerated to an energy of 13 MeV by the plane wave transformer (PWT) accelerating cavity. The third and fourth dipole magnets of a chicane compressor are used as a 45-degree bend (yellow wedge) to divert the beam onto the dogleg section, which has been named $S - Bahn$, after a train system in Hamburg, Germany. The dogleg has a negative longitudinal dispersion (or R_{56}), which can be utilized to generate a partial compression of the beam as shown in Fig. 1 and thereby produce a ramp-shaped profile. A second pair of dipoles (second yellow wedge) bends the beam trajectory back by 45 degrees onto a path which runs parallel to, but horizontally displaced from, the original photoinjector beamline. This parallel beamline has a triplet of traditional electromagnetic quadrupole magnets followed by a diagnostic section. Two alternative diagnostic setups will be employed, as shown in the inset in Fig. 2. Setup 1 will consist of a triplet of permanent magnet quadrupoles followed by a Ce:YAG profile monitor, which will be used to obtain a high-brightness focus, as discussed in the Introduction. Setup 2 will employ a 9-cell X-Band dipole mode deflecting cavity, the final version of which is

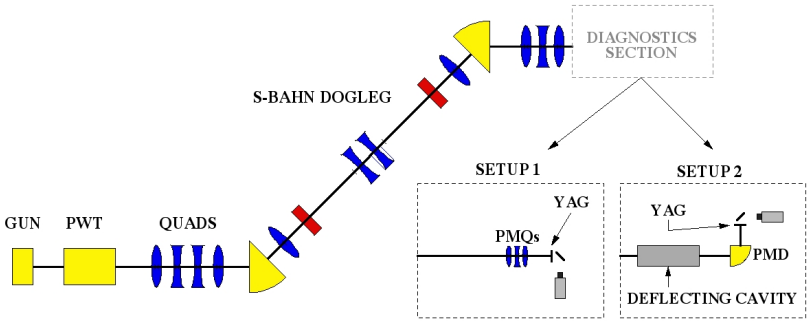

Figure 2. Cartoon graphic of the experimental beamline (not to scale). Blue lenses, red rectangles, and yellow wedges represent quadrupoles, sextupoles, and dipole magnets respectively. Two alternate setups are shown for the final diagnostics section.

currently under construction. The deflecting cavity will serve as a temporal diagnostic to measure the current profile of the beam for comparison with simulation results such as those shown in Fig. 1. As the deflecting cavity diagnostic is the subject of a recent conference paper,[10] we will concentrate primarily on the details of Setup 1 in the following sections.

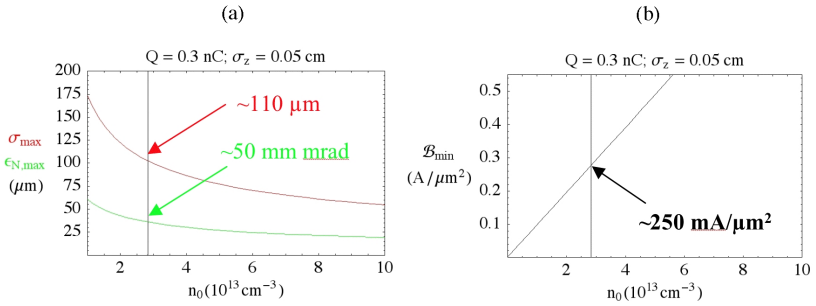

Figure 3. Plot of the constraints as given by Eqns. (1)-(4), with approximate maximal values for beam size and emittance, and minimum brightness.

Using the constraints on the beam parameters imposed by Eqs. (2)-(3), we can construct plots showing the maximum allowable beam size and emittance as a function of plasma density n_0 for a 0.5 mm long 300 pC beam. This is shown in Fig. 3(a). Combining this with the minimum density of $n_0 = 2.8 \times 10^{13} cm^{-3}$ required by Eq. (1) gives us estimated

upper limits on RMS beam size and normalized emittance of 110 μm and 50 mm mrad respectively. A corresponding plot of minimum brightness using Eq. (4), shown in Fig. 3(b), gives a lower limit of 250 $mA/\mu m^2$. These limits are compared with simulation results in Section 2.3.

2.2. *Permanent Magnet Quadrupoles*

The permanent magnet quadrupoles (PMQs) to be used for the S-Bahn final focus shown in Setup 1 of Fig. 2 are compact, with a high magnetic field gradient, making them useful for focusing of high-brightness space-charge dominated beams such as those produced at the Neptune laboratory. The magnets incorporate a hybrid iron and permanent magnet design originally developed for the nonlinear inverse Compton scattering experiment that is currently in progress at the Neptune laboratory.[11] The magnets, shown in Fig. 4, contain cubes of NdFeB, surrounded by an iron yoke which serves to close the magnetic circuit. Four hyperbolic pole faces constructed by wire electric discharge machining (EDM) are held against the NdFeB cubes in a quadrupole array around the geometric center by an aluminum keeper.

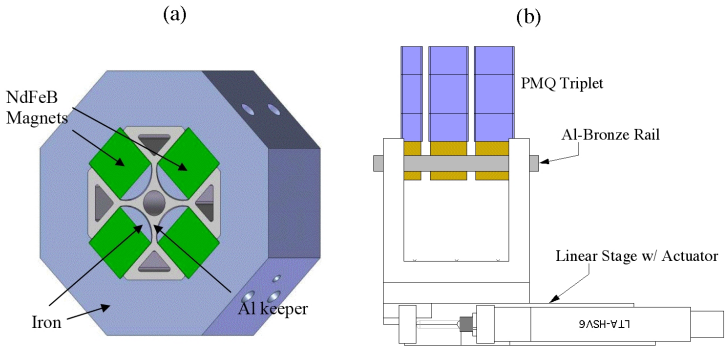

Figure 4. Drawing of hybrid permanent magnet quadrupole design (a), courtesy of A. Doyuran, *et al.*[12], and schematic of assembled triplet and stand (b).

Magnets of 1 cm and 2 cm lengths have been constructed, incorporating 4 and 8 NdFeB cubes respectively. The measured field strengths of the two types are similar (109 and 110 T/m respectively). The proposed configuration for the triplet is a single 1 cm length defocusing PMQ, followed by a focusing and then a defocusing 2 cm long PMQ. A side view of the

assembly is shown in Fig. 4 (b) at a reduced scale.

2.3. *Simulations of Experimental Results*

The PMQ focusing system described in Section 2.2 was simulated initially using the matrix-based beam envelope code PowerTrace. Further studies were then done using the particle tracking code ELEGANT to model the dogleg and final focus sections.[12] The phase space coordinates for the particles used as the input for the ELEGANT simulation were generated by a UCLA-PARMELA simulation of the photoinjector and linac.

Simulated experimental values for energy E, charge Q, normalized emittances $\epsilon_{x,N}$ and $\epsilon_{y,N}$, RMS bunch length and transverse dimensions σ_t, σ_x, σ_y, and brightness B are given in Table 1. Initial values correspond to the beam parameters immediately after the accelerating section, and final values correspond to the final focus location of the permanent magnet quadrupole triplet of Setup 1. Final values represent design goals based upon the PARMELA and ELEGANT simulation results. The shape of the longitudinal phase space predicted by these simulations was shown previously in Fig. 1. The reduction in charge is a prediction based upon observed transportation losses in the beamline, and the emittance growth is due primarily to transverse nonlinear effects in the dogleg. Note that the predicted beam sizes, emittance values, and brightness fall roughly within the limits set by Eqs. (1)-(4), as discussed in Section 2.1, for applicability to plasma wake-field studies with large transformer ratios.

Table 1. Simulated Experimental Parameters

Parameter	*Initial*	*Final*	*Units*
E	13	13	MeV
Q	300	240	pC
$\epsilon_{x,N}$	5	41	mm mrad
$\epsilon_{y,N}$	5	15	mm mrad
σ_t	2.5	1.8	ps
σ_x	1	0.130	mm
σ_y	1	0.057	mm
B	7600	433	mA/μm^2

3. Future Directions

3.1. *Creation of a Witness Bunch*

In order for the ramped bunch mechanism described in Section 1 to represent a useful technology for the wake-field accelerator, it must be compatible with some feasible scheme for creating a witness bunch. The witness bunch would ideally be a bunch of much lower charge which trails behind the main drive bunch, and can therefore be accelerated by the wake-fields which are generated by the drive bunch. One technique used in the past has been to accelerate the tail of the drive bunch itself. However, the mechanism described in Section 1 is designed to create a drive bunch with a sharp cutoff at the tail end, as seen in Fig. 1(c). We see, however, in Fig. 1(b), that with the sextupole correctors turned off, the nonlinear effects produce a significant lower-energy tail behind the bunch, but the ramped shape is lost. A potential solution would be to operate in a regime intermediate be-

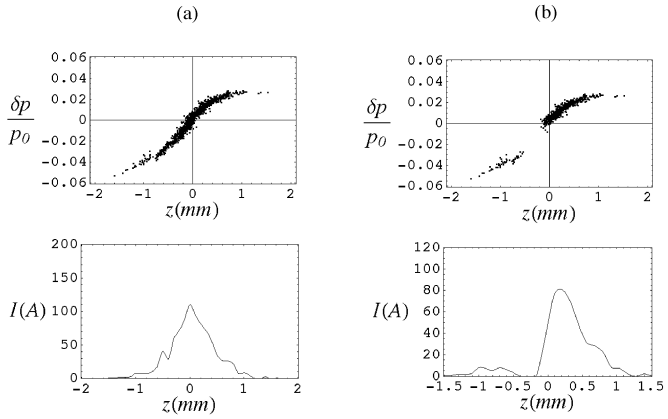

Figure 5. Simulation of undercorrected beam at exit of dogleg with collimator removed in (a) and inserted in (b), thereby producing a ramped drive beam followed by a low-charge witness bunch.

tween the conditions represented in Fig.2(b) and 2(c), where the sextupole magnets are turned on but at a lower field strength, producing a beam with a ramp at the front followed by a more tapered fall-off at the back. This situation is seen in Fig.5(a), which shows the results of an ELEGANT simulation of the dogleg compressor. By inserting a 1 cm wide collimator in

the x-direction, at a location in the dogleg (corresponding to the position of the quadrupole before the final dipole in Fig. 2) where the horizontal dispersion is large and therefore there is a strong correlation between x and z, the tail of the beam can be truncated from the main body. As shown in Fig. 5(b) this results in a ramp-shaped primary bunch followed by a separate trailing bunch of lower charge. This scheme has the benefit of being relatively simple, requiring only the insertion of a collimator into the beamline. However, the resultant reduction in charge and horizontal truncation of the beam must be taken into consideration in the design of the downstream focusing optics.

3.2. *Scaling to High Charge: 4 nC*

Future upgrades to the Neptune laboratory, including a new drive laser oscillator, replacement of the photoinjector, photocathode laser cleaning, and higher RF power levels in the gun are expected to increase the bunch charge to as high as 4 nC. It is therefore of interest to consider how the bunch shaping mechanism described previously scales to higher charge. Preservation of the beam envelope under the emittance compensation mechanism in the gun and linac requires that the bunch dimensions at the cathode scale with charge as $Q^{1/3}$. This scaling is accomplished by stretching the pulse length of the photocathode drive laser and expanding its transverse dimensions accordingly. Simulations of the Neptune photoinjector under this scaling in UCLA-PARMELA indicate a normalized emittance of $\epsilon_{x,N} = \epsilon_{y,N} = 25$ mm mrad at the exit of the linac with 4% transportation losses for an initial charge of 4 nC. Since the dogleg compression mechanism requires a chirped beam, the bunch was chirped in energy by setting the RF phase of the linac in the simulation to a value corresponding to an injection phase of 22 back of crest. This chirp, and the increase in bunch length due to the charge

Table 2. Simulated Parameters Corresponding to Fig. 6 (a), (b), and (c)

Parameter	(*a*)	(*b*)	(*c*)	*Units*
$\epsilon_{x,N}$	742	96	46	mm mrad
$\epsilon_{y,N}$	456	141	68	mm mrad
T_{166}	-0.26	0.00	-0.26	m
T_{266}	-7.9	0.00	-7.9	rad
T_{566}	-0.04	0.623	-0.04	m
U_{5666}	-2.44	-1.02	-2.44	m

scaling, result in a predicted 4.5% RMS energy spread, compared with 1.8% energy spread for the 300 pC case.

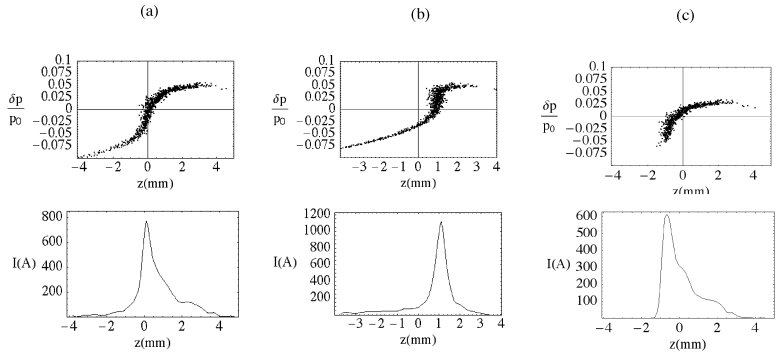

Figure 6. Simulation of longitudinal phase space and current profiles of 4nC beam at exit of dogleg compressor with (a) with sextupoles set to eliminate second-order longitudinal dispersion (T_{566}), (b) with sextupoles set to eliminate second-order horizontal dispersion (T_{166}), and (c) with sextupoles set as in part (a) but with a collimator inserted to remove low-energy tail.

The final phase space coordinates of the particles in the PARMELA simulation were then used as the input for an ELEGANT simulation of the dogleg compressor. The results of these simulations indicated that due to the larger energy spread of the 4 nC beam, two undesirable effects became more pronounced: (1) distortion of the longitudinal phase space by third-order longitudinal dispersion (U_{5666} in transport notation) and (2) emittance growth due to horizontal second-order dispersion (T_{166} and T_{266}). The first effect results in the formation of a low-energy tail behind the beam. This is seen in Fig.6(a). The tail can, in principle, be corrected by the use of octupole magnets. The second effect requires the use of sextupole magnets and is somewhat more difficult to remedy, due to the fact that, at least for the particular optical configuration of the Neptune dogleg, it is impossible to simultaneously eliminate both the horizontal and longitudinal second order dispersion (T_{166} and T_{566} respectively). Consequently, the sextupole magnets may be used to eliminate the second order horizontal dispersion, thereby improving the final emittance, but as a result the longitudinal dispersion becomes nonzero and so the shape of the ramped profile is destroyed. This scenario is illustrated in Fig. 6(b). A solution

which appears to solve both problems is to simply eliminate the tail in part (a) by collimating the beam. As it turns out, much of the emittance growth is due to the low-energy particles contained in this tail, and their removal improves the final emittance by a factor of two and restores the ramped profile, as seen in Fig. 6(c). By using a collimator of finite width, a small subset of the tail particles could be left as a witness bunch, making this technique compatible with the results of the previous section. To clarify these results, the simulated emittance and corresponding matrix element values are provided in Table 2.

It should be noted that the simulations above do not include transmission losses due to ordinary apertures of the beamline. And in fact, the simulated RMS beam sizes in the dogleg for the high-charge case are found to exceed the radius of the beam pipe. Consequently, although scaling the compressor to higher charge appears theoretically feasible, it would, in practice, be necessary to expand the apertures of the beamline, which would require a significant redesign of the beamline hardware.

4. Conclusions

We have described an experiment underway at the Neptune laboratory to create 300 pC electron bunches 1 to 2 ps in duration with a linearly ramped current profile suitable for use as a plasma wake-field drive beam. To obtain a final beam of sufficiently high brightness, a final focusing system has been constructed, incorporating a triplet of hybrid permanent magnet and iron quadrupoles. Simulation results using PARMELA and ELEGANT predict that the final transverse beam brightness and normalized emittances (450 mA/μm^2 and 100 μm respectively) should be within the limits required for generation of large-amplitude (transformer ratio >2) wake-fields. Simulations also indicate the feasibility of a proposed method for creating a witness beam, by undercompressing the beam slightly in the dogleg and severing the resulting low-energy tail from the main body of the beam using an insertable collimator. In addition, the feasibility of scaling the beam-shaping scheme to high charge (4 nC) was studied. Simulations of the high-charge case indicate that undesirable emittance growth and phase space distortion produced as a result of the larger energy spread can largely be corrected by truncation of low-energy particles using collimation. However, the larger beam size exceeds the apertures of the beamline and would most likely require significant redesign of the existing hardware.

References

1. J. B. Rosenzweig. Acceleration and focusing of electrons in two-dimensional nonlinear plasma wake fields. *Phys. Rev. A*, 44:R6189–6192, November 1991.
2. P. Muggli, B. E. Blue, C. E. Clayton, S. Deng, F. J. Decker, M. J. Hogan, C. Huang, R. Iverson, C. Joshi, T. C. Katsouleas, S. Lee, W. Lu, K. A. Marsh, W. B. Mori, C. L. O'Connell, P. Raimondi, R. Siemann, and D. Walz. Meter-Scale Plasma-Wakefield Accelerator Driven by a Matched Electron Beam. *Phys. Rev. Lett.*, 93:014802, June 2004.
3. N. Barov, J. B. Rosenzweig, M. E. Conde, W. Gai, and J. G. Power. Observation of plasma wakefield acceleration in the underdense regime. *Phys. Rev. ST-AB*, 3:011301, January 2000.
4. N. Barov, J. B. Rosenzweig, M. C. Thompson, and R. B. Yoder. Energy loss of a high-charge bunched electron beam in plasma: Analysis. *Phys. Rev. ST-AB*, 7:061301, June 2004.
5. K. L. F. Bane, Pisin Chen, and P. B. Wilson. On Collinear Wake Field Acceleration. Technical Report SLAC PUB-3662, Stanford Linear Accelerator Center, Stanford, CA 94305, April 1985.
6. T. Katsouleas. Physical Mechanisms in the Plasma Wake-Field Accelerator. *Phys. Rev. A*, 33:2056–2064, March 1986.
7. K. V. Lotov. Efficient operating mode of the plasma wakefield accelerator. *Physics of Plasmas*, 12:053105, May 2005.
8. R. J. England, J. B. Rosenzweig, G. Andonian, P. Musumeci, G. Travish, and R. Yoder. Sextupole Correction of the Longitudinal Transport of Relativistic Beams in Dispersionless Translating Sections. *Phys. Rev. ST-AB*, 8:12801, January 2005.
9. L. Young and J. Billen. PARMELA. Technical Report LA-UR-96-1835, Los Alamos National Laboratory, Los Alamos, NM, 1996.
10. R. J. England, B. O'Shea, J. B. Rosenzweig, G. Travish, and D. Alesini. X-band dipole mode deflecting cavity for the UCLA Neptune beamline. In *Proceedings of the 2005 Particle Accelerator Conference*, IEEE, page 2627, 2005.
11. A. Doyuran, O. Williams, R. J. England, C. Joshi, J. Lim, J. B. Rosenzweig, S. Tochitsky, and G. Travish. Investigation of x-ray harmonics of the polarized inverse compton scattering experiment at UCLA. In *Proceedings of the 2005 Particle Accelerator Conference*, IEEE, pages 2303–2305, 2005.
12. M. Borland. ELEGANT: A Flexible SDDS-Compliant Code for Accelerator Simulation. Technical Report LS-287, Argonne National Laboratory Advanced Photon Source, Argonne, IL, September 2000.